

Chaos Control for Power Converters

Ilse Cevantes¹, IEEE member and Jose Alvarez-Ramirez²

¹Seccion de Estudios de Posgrado e Investigacion, ESIME-CU Av. Santa Ana 1000, Col. San Francisco Culhuacan, México D.F. 04430 MEXICO. email: ilse@calmecac.esimecu.ipn.mx.

² Univesidad Autonoma Metropolitana Iztapalapa.CBI email: jjar@xanum.uam.mx

Abstract- In this work, the boost converter has been taken as a benchmark to show how a simple control law can lead to chaos elimination and equilibrium point stabilization. In this way, we have shown that its possible to design a linear feedback controller that ensures the stability and reliability of the system under the action of current programmed control (CPC) or voltage programmed control (VPC). The proposed strategy has the advantages of being simple, efficient and easy to implement. Furthermore, the proposed controller does not require any information about unstable periodic orbits of the system. Performance and robustness of the controller are evaluated via numerical simulations. Limitations of the proposed strategy are discussed.

I. INTRODUCTION

Power converters constitute today, a main tool in energy processing. Recently, it has been shown that DC-DC converters can exhibit several types of nonlinear phenomena including bifurcation, quasiperiodicity and chaos, under voltage and current mode control schemes (see for example Barnejee and Verghese, 2001). Because of the unpredictable and undesirable consequences of chaos, control of chaos, and in particular control of chaos in DC-DC converters, has become a topic of interest.

There exist in the literature several approaches to chaos control. The first chaos control strategy was reported by Ott-Grebogi-Yorke (OGY) (1990). The main idea is to use small perturbations to stabilize unstable periodic orbits (UPO) which are abundant in chaotic attractors. In this way, one of many UPOs is identified as the control target and control action is directed to stabilize the system around the specific orbit. Unfortunately, the implementation of the OGY method requires of the computation of the UPO which may be in general a very complex task. To overcome this problem two strategies has been proposed: Occasional proportional feedback (OPF) introduced by Hunt (1991) and the so

called time-delayed autosynchronization (TDAS) suggested by Pyragas (1992). OPF method (Hunt, 1991; Petrov et al, 1992) is a one-dimensional version of OGY and has the advantage of non-requiring the exact value of the unstable periodic point or eigenvalues. On the other hand, TDAS method involves a control action formed with the difference between the actual state and the state delayed of the system by one period. In this way, the computation of the periodic orbit is avoided but substituted by the exact period of the UPO. Given the complexity of computing information about UPOs, another kind of control strategies have been proposed. In these control schemes, the control target is a desired operating state, not necessarily an UPO (Huberman and Lumer, 1990; Cicogna,1990; Braiman & Goldhirsh, 1991). Such controllers have the disadvantage of being constituted mainly by non-feedback stabilizers and therefore, they are non-robust to system disturbances. On the other hand, chaos control strategies of power converters found in literature, are mainly direct applications of the chaos control methodologies given above and do not exploit system particularities to accomplish the stabilization task.

In this paper, the chaos control of DC-DC power converters under CPC and VPC is investigated. It is shown that is possible to design simple feedback controllers to eliminate chaotic behavior in converters, so stability and reliability of the system can be ensured. To this end, we take the boost converter as a benchmark to study the chaos generation and to develop a discrete-time model for control purposes. The proposed strategy has the advantage of being simple, easy to implement and does not requires of any information about UPOs or about location of equilibrium points. Mainly, the contribution of this note, is to introduce a systematic procedure to design simple control laws for a class DC-DC power converters, that eliminate chaotic behavior and stabilize an equilibrium set. The stabilizing task is perfomed exploiting the particular dynamics of the converter. The performance and robustness of the control scheme in presence of parameter uncertainty is evaluated via numerical simulations.

This note is organized as follows. Section 2 describes the converter dynamics under the current programmed controller. Section 3 is aimed at develop a discrete-time model of the system for analysis and control purposes, and states formally the chaos control problem. Section 4 analyze the conditions for the existence of fixed points, Section 5 presents the controller design and provides a rigorous proof of stability. Section 6 illustrates the performance of the controller via numerical simulations and finally, in Section 7 some conclusions are presented. **Notations.** Throughout this paper, $|\cdot|$ denotes the Euclidean norm, $\|\cdot\|$ denotes the induced matrix norm and $\nabla_x s(x)$ denotes the gradient (Jacobian) of the scalar (vector) function $s(x)$. For a given matrix \mathbf{A} , $\lambda(\mathbf{A})$ denotes the matrix eigenvalues, respectively. The symbol \mathbf{x}^{Tr} denotes the transpose of vector \mathbf{x} . The symbol I_n represents the n -dimensional identity matrix.

II. PRINCIPLE OF OPERATION

As a first step towards addressing the problem of reducing the adverse chaos effect in power converters, a simple benchmark system is analyzed. In this way, consider the boost converter shown in Figure 1, which consists of a switch S , a diode D , a capacitor C , an inductor L and a load resistor R in parallel with the capacitor. Current mode control is consider for analysis purposes, however, the results derived for this case can also be extended for voltage mode, as shown in following sections. In current programmed control, Switch S is controlled by a feedback path that consists of a flip-flop and a comparator. In the beginning, a clock pulse at the Set input of the latch initiates the switching period, causing the latch output Q to be high and turning on the transistor (switch conducts). While the transistor conducts, its current is equal to the inductor current $i_L(t)$, this current increases depending the value of the inductance L and the capacitance C . Any pulse arriving during this period of time is ignored. Eventually the inductor current reaches the reference current I_{ref} . At this point, the controller turns the transistor switch off, and the inductor current decreases for the remainder of the switching period. That is, when $i_L(t) = I_{ref}$ the comparator is triggered to reset the clock pulse. The switch S is opened and remains open until the arrival of the next clock pulse which triggers S to conduct again. Summarizing, the current programmed control is constituted of two switching criterions: 1) A unconditional close (S conducts) every time period T , 2) A conditional open (S does not conduct) whenever $i_L(t) \geq I_{ref}$.

An advantage of the current programmed control is that it makes use of the available current sensor information to obtain simpler input-output dynamics. Furthermore, transistor failures due to excessive switch op-

eration can be prevented simply by limiting the maximum reference current. This ensure that the transistor will turn off whenever the switch current becomes to large. On the other hand, current programmed control is essentially an analogic technique, and their accuracy and response speed are often better for current control in highly demanding applications, than those based in digital technology (Malesani, et al 1997).

As can be noticed, the topology of the converter is changed according to the *on* or *off* state of the switch. This results in a nonlinear time-varying system. There are two particular useful modeling approaches for this type of switched converters: Continuous-time averaging approach and discrete time iterative map approach. The averaging approach usually leads to continuous non-linear equations that are more likely mathematical tractable, however, the averaging method is not adequate for those cases when relative low frequency excitation of the switch is used. On the other hand, discrete-time maps offer more complete information on the dynamical behavior of the system, since they can reflect nonlinear phenomena across a wide spectrum of frequency. Furthermore, the discrete time models can be applied to a more general class of hybrid systems as piecewise linear time variant systems. Given the arguments above, in this paper we develop a discrete time map of the system. Notice that since the switching exhibited by the converter is modulated by a signal of period T , a synchronous map of the system seems to be the more adequate.

III. DISCRETE MODEL OF THE CONVERTER

In order to derive a discrete time map of the boost converter, let us assume that the circuit is evolving on a continuous conduction mode, that is, the inductor current never falls to zero. In this case, the equations describing the *on* switching stage (S conducts) are two uncoupled first order differential equations, one for the inductor current and one for the capacitor voltage:

$$\begin{bmatrix} \frac{dv}{dt} \\ \frac{di_L}{dt} \end{bmatrix} = A_{ON} \begin{bmatrix} v \\ i \end{bmatrix} + \begin{bmatrix} 0 \\ \frac{E}{L} \end{bmatrix} \quad (1)$$

where $A_{ON} \stackrel{def}{=} \text{diag} \left[-\frac{1}{RC}, 0 \right]$. In this stage, the capacitor voltage decreases and the inductor current raises linearly until the inductor current reaches the reference current I_{ref} . At that time, the switch is opened and the converter evolves in a the non-conduction mode given by

$$\begin{bmatrix} \frac{dv}{dt} \\ \frac{di_L}{dt} \end{bmatrix} = A_{OFF} \begin{bmatrix} v \\ i \end{bmatrix} + \begin{bmatrix} 0 \\ \frac{E}{L} \end{bmatrix} \quad (2)$$

where $A_{OFF} \stackrel{def}{=} \begin{bmatrix} -\frac{1}{RC} & \frac{1}{C} \\ -\frac{1}{L} & 0 \end{bmatrix}$ is an invertible and Hurwitz matrix since $R, C, L > 0$. At this point, notice that in view of the philosophy of current programmed control, there may be two typical behaviors:

Case a. The switch is turned off during the time T ,
or

Case b. The switch remains closed since the current condition $i_L(t) = I_{ref}$ is not satisfied over the time period T .

A. The off switching condition is satisfied

In this case, the switch is both turned *on* and *off* during the time period T . The typical current waveform is shown in Figure 2.a. Let δ_n be the fraction of time that switch remains closed, then the state vector at the *off*-switching time is the following:

$$x'_n = \Psi(\delta_n T)x_n + \beta_E \delta_n T \quad (3)$$

where $x = [v, i_L]^{Tr}$, $\beta_E = [0, \frac{E}{L}]^{Tr}$, $\Psi(\delta_n T) = \text{diag}[\varphi, 1]$, $\varphi(\delta_n) \stackrel{def}{=} e^{-\frac{\delta_n T}{RC}}$ and x_j is the vector state at the instant jT . Notice that since the dynamics of the states are decoupled, the matrix $\Psi(\delta_n T)$ is diagonal. On the other hand, the converter at instant T is given by

$$x_{n+1} = e^{A_{OFF}(1-\delta_n)T} x'_n + A_{OFF}^{-1} [e^{A_{OFF}(1-\delta_n)T} - I] \beta_E$$

In this way, the overall map $x_n \rightarrow x_{n+1}$ is a composed map given by

$$x_{n+1} = e^{A_{OFF}(1-\delta_n)T} [\Psi(\delta_n T)x_n + \beta_E \delta_n T] + A_{OFF}^{-1} [e^{A_{OFF}(1-\delta_n)T} - I] \beta_E \stackrel{def}{=} L_a(x_n, \delta_n) \quad (4)$$

Notice that the discrete function (4) is non-linear since the parameter δ_n (duty-cycle) depends on the initial conditions x_n .

B. The switch remains on

In this case, the switch remains open since the current does not reach the reference over a time period T . The current waveform is shown in Figure 2.b. The discrete map between the instant nT and $(n+1)T$ is given by

$$x_{n+1} = \Psi(T)x_n + \beta_E T \stackrel{def}{=} L_b(x_n) \quad (5)$$

IV. EXISTENCE OF FIXED POINTS

Since fixed points are related with the equilibrium of discrete systems, we explore the conditions for their existence in this section. In this way, consider first the Case b in section above (Figure 2.b). There exists a fixed point in map (5) if

$$\begin{aligned} v_n &= e^{-\frac{T}{RC}} v_n \\ i_n &= i_n + \frac{E}{L} T \end{aligned} \quad (6)$$

Eq (6) cannot be satisfied unless $T = 0$. This situation would correspond to a non-operating converter and therefore there are not fixed points. This situation lead us to think that if a fixed point exists, it would be in the composed map $L_a(x_n, \delta_n)$ (4). This is not surprising, since the OFF-stage of the converter is necessary to dissipate all the energy stored by the inductor in the ON-stage. In this way, there is a fixed point if the following is satisfied

$$x_n = e^{A_{OFF}(1-\delta_n)T} [\Psi(\delta_n T)x_n + \beta_E \delta_n T] + A_{OFF}^{-1} [e^{A_{OFF}(1-\delta_n)T} - I] \beta_E \quad (7)$$

As remarked above, Eq. (7) is a nonlinear and transcendental function. The solution of this equation is not an easy matter and is probably that it has multiple solutions. However, notice that for a given constant duty cycle δ^* the vector state is given by

$$x_n = e^{A_{OFF}(1-\delta^*)T} [\Psi(\delta^* T)x_n + \beta_E \delta^* T] + A_{OFF}^{-1} [e^{A_{OFF}(1-\delta^*)T} - I] \beta_E \quad (8)$$

Eq. (8) is linear and therefore a sufficient condition for the existence of a fixed point is that the matrix $I - e^{A_{OFF}(1-\delta^*)T} \Psi(\delta^* T)$ be invertible. Let us, for simplicity, denote as α_{ij} the entries of matrix $e^{A_{OFF}(1-\delta^*)T}$. Then the condition of invertibility can be translated as

$$1 - \varphi\alpha_{11} - \alpha_{22} + \varphi(\alpha_{11}\alpha_{22} - \alpha_{12}\alpha_{21}) \neq 0 \quad (9)$$

Restriction (9) is satisfied if A_{OFF} is Hurwitz and $0 < \varphi < 1$, the proof can be found in later sections. Hence, there exists a fixed point x_n for every constant duty-cycle δ^* . At this point, it is worth noticing that since the erratic behavior of the converter is originated by a random variable duty cycle, the use of a constant pulse width would in principle eliminate chaos. In this way, one may think in changing the reference current to accomplish a constant duty-cycle operation. To this end, let us notice that from Eq. (3), the restriction on the reference output satisfies

$$y_{ref} = c\Psi(\delta^* T)x_n + c\beta_E \delta^* T \quad (10)$$

where $y = cx$ and $c = [0, 1]^T$ for current programmed control. Eq. (10) can be simplified to the following expression

$$I_{ref} = i_n + \frac{E}{L} \delta^* T \quad (11)$$

Notice that for every δ^* there is one and only one I_{ref} . If I_{ref} is defined as a control variable, Eq. (11) constitutes a discrete control law that makes use information of the inductor current at every instant nT . It can be proved that control law (10) (alternately (11)) leads to asymptotic stability of the closed-loop system. This result is formalized in following Section and constitutes the main result of this note. As a preliminary step of this proof, consider the following results.

Lemma 1 (Chen, 1999). *Let P be a Hurwitz matrix, then e^P is Schur.*

Lemma 2 *Let $e^P \in \mathbb{R}^2$ be a Schur matrix and $\Pi = \text{diag}[\pi, 1]$ with $0 < \pi < 1$, then $e^P \Pi$ is Schur.*

Proof. Let p_{ij} denote the entries of e^P , then its characteristic equation is given by $f_1(\lambda) = \lambda^2 - (p_{11} + p_{22})\lambda + p_{11}p_{22} - p_{12}p_{21}$. Since the matrix e^P is Schur it satisfies the following (Chen, 1999)

$$\begin{aligned} 1 - p_{11} - p_{22} + p_{11}p_{22} - p_{12}p_{21} &> 0 \\ 1 + p_{11} + p_{22} + p_{11}p_{22} - p_{12}p_{21} &> 0 \\ p_{11}p_{22} - p_{12}p_{21} &< 1 \end{aligned} \quad (12)$$

furthermore since $\det(e^P) = e^{\text{trace}(P)} > 0$, $0 < \det(e^P) < 1$. Therefore, from (12) one can see that p_{11} satisfies

$$-2 - p_{22} < p_{11} < 2 - p_{22}$$

On the other hand, the characteristic equation of $e^P \Pi$ is given by

$$f_2(\lambda) = \lambda^2 - (\pi p_{11} + p_{22})\lambda + \pi(p_{11}p_{22} - p_{12}p_{21})$$

which is Schur if satisfies

$$\begin{aligned} 1 - \pi p_{11} - p_{22} + \pi(p_{11}p_{22} - p_{12}p_{21}) &> 0 \\ 1 + \pi p_{11} + p_{22} + \pi(p_{11}p_{22} - p_{12}p_{21}) &> 0 \\ \pi(p_{11}p_{22} - p_{12}p_{21}) &< 1 \end{aligned} \quad (13)$$

Since $0 < \pi < 1$ the last restriction in (13) is satisfied. On the other hand, (13) implies that $\frac{-2-p_{22}}{\pi} < p_{11} < \frac{2-p_{22}}{\pi}$. Notice that since $\frac{-2-p_{22}}{\pi} < -2 - p_{22}$, $\frac{2-p_{22}}{\pi} > 2 - p_{22}$ (13) is satisfied, leading us to conclude that matrix $e^P \Pi$ is Schur. This concludes the proof ■

Remark 1 *From Lemma 2, one can also conclude the existence of a fixed point in map (8). Since restriction the satisfaction of restriction (13) guarantees the satisfaction of (9).*

V. MAIN RESULT

The main contribution of this note is presented below in the following theorem

Theorem 3 *Consider the converter dynamics under current programmed control and the feedback expression (10), then the closed-loop system is globally asymptotically stable about the equilibrium point*

$$\begin{aligned} x &= [I - e^{A_{OFF}(1-\delta^*)T} \Psi(\delta^*T)]^{-1} [e^{A_{OFF}(1-\delta^*)T} \beta_E \delta^*T \\ &+ A_{OFF}^{-1} [e^{A_{OFF}(1-\delta^*)T} - I] \beta_E \end{aligned} \quad (14)$$

Proof. The closed loop equations are given by

$$\begin{aligned} x_{n+1} &= e^{A_{OFF}(1-\delta^*)T} \Psi(\delta^*T) x_n + e^{A_{OFF}(1-\delta^*)T} \beta_E \delta^*T \\ &+ A_{OFF}^{-1} [e^{A_{OFF}(1-\delta^*)T} - I] \beta_E \end{aligned} \quad (15)$$

Notice that the stability of the discrete-time system (15) is ensured if the matrix $e^{A_{OFF}(1-\delta^*)T} \Psi(\delta^*T)$ is Schur. Since $(1 - \delta^*)T > 0$, the result in Lemma 1 implies that matrix $e^{A_{OFF}(1-\delta^*)T}$ is Schur. From Lemma 2, one can conclude that $e^{A_{OFF}(1-\delta^*)T} \Psi(\delta^*T)$ is also Schur, since $0 < \varphi < 1$. Therefore system (15) is globally asymptotically stable about the equilibrium point (14). The existence of such equilibrium is guaranteed since, as shown before, matrix $I - e^{A_{OFF}(1-\delta^*)T} \Psi(\delta^*T)$ is invertible. This concludes the proof ■

Remark 2 *Result in Theorem 3 establish that by defining the reference as in (10), any possible erratic behavior of the system under current programmed control is eliminated. Even more, the result presented in this note is also valid for voltage programmed control (VPC) just by defining the output vector in (10) as $c = [1, 0]^T$.*

Remark 3 *Although system stability under CPC or VPC is ensured by feedback control law (10), the regulation voltage problem is not necessary solved. However, given that for every δ^* there exists one and only one fixed point x , one can follow the methodology given in (Cervantes et al 2003, Alvarez et al. 2002) to design an outer-loop in order to obtain a desired output voltage.*

Remark 4 *As stated before, Theorem 3 establish the conditions to derive global asymptotic stability of the converter under control law (10) to the fixed point (14). At this point, one may wonder if this result is preserved in presence of parametric uncertainty. Deriving a formal stability result of this case is quite involved, however as we will see later, the control law (10) is able to stabilize the system even if the parameters are uncertain. This fact is illustrated via numerical simulations in Section above.*

Remark 5 *Given the linear nature of the control law (10) it can be easily implemented. In principle, such circuit would require of an operational amplifier and a "sample and hold" circuit.*

VI. NUMERICAL STUDIES

In order to illustrate the performance and robustness of the proposed controller, numerical simulations were carried on a boost converter with the following parameters: $R = 10\Omega$, $L = 0.5mH$, $C = 4\mu F$, $I_{ref} = 7$, Amp , $T = 50\mu s$ and $E = 5V$. It has been shown that for this parameters the boost converter displays erratic, presumable chaotic behavior (Barnerjee and Verghese, 2001). This fact is illustrated in Figure 3. On the other hand, in order test the efficacy of the proposed controller, the following experiment was performed. The converter is let to evolve freely and then at time $t = 0.0025s$ the feedback control law (10) is activated. Figure 4 shows the time evolution of the voltage capacitor and the inductor current for this case and $\delta^* = 0.5$. It can be noticed that the controller is able to eliminate the erratic behavior, stabilizing the converter to a fixed point. In this way, as stated in Theorem 3, all trajectories $x(t, x_0)$ of the converter system are trapped by an equilibrium set, stabilizing the system.

To guarantee the stability result in Theorem 3, the control action (10) requires the knowledge of circuit parameters. At this point, one may wonder if the result can be preserved in presence of parametric uncertainty. As stated before, deriving a formal stability result of this case is quite involved, however one may test its robustness via numerical simulations. To this end, the control law (10) was tested with a parametric uncertainty of $\pm 20\%$; that is, $L = 0.6mH$, and $E = 4V$. The results are shown in Figure 5. It can be noticed that the controller is able to stabilize the system even in presence of parametric uncertainty and the system trajectories are attracted to a fixed point.

VII. CONCLUSIONS

The main conclusion of this Letter is that by analyzing the dynamics of DC-DC converter under CPC or VPC, it can be possible to design simple feedback controllers to eliminate chaotic behavior. Advantages of proposed controller are its simplicity, efficiency and easy implementation. More specifically, we have used boost converter as a benchmark to show how a suitable the control law can lead to chaos elimination and equilibrium point stabilization. A salient feature of the proposed control strategy is that information on the location of equilibrium points is not required. In this way, strategies similar to the presented in this paper could be tested to reduce the adverse effects of chaotic converters in other kind of DC-DC converters, like buck and buck-boost.

VIII. REFERENCES

- [1] S. Barnerjee, G.C. Verghese. Nonlinear Phenomena in Power Electronics: Bifurcations, Chaos, Control and Applications. IEEE Press., 2001.
- [2] E. Ott, C. Grebogi, J. Yorke, (1990) "Controlling chaos", Phys Rev Lett, 1990, vol. 64 no.11 pp.1196-1199.
- [3] E. R. Hunt, "Stabilizing high-period orbits in chaotic system: The diode resonator" Phys. Rev. Lett. vol 67 no. 15, pp. 1953-1955, 1991
- [4] K.Pyragas, (1992) "Continuous control of chaos by self-controlling feedback," Physics Letters A 170, 421-428
- [5] V. Petrov, B. Peng and K. Showalter, (1992) "A map-based algorithm for controlling low-dimensional chaos" J. Chem. Phys. vol 96, nos 10/15, pp. 7506-7513,
- [6] B.A. Huberman and E. Lumer, (1990) "Dynamics of adaptive systems", IEEE Trans. Circuits Syst.-I vol 37, pp. 547.550.
- [7] G. Cicogna,(1990) "Changing the threshold of chaos in multimode solid state lasers by the use of small periodic perturbations" Phys. Rev. E, vol 53, pp. 200-206.
- [8] Y. Braiman and I.Goldhirsh, (1991) "Taming chaotic dynamics with weak periodic perturbations" Phys. Rev. Lett. vol 66, pp.2545-2548.
- [9] L. Malesani, P. Mattavelli and P. Tomasin, (1997) "Improved constant-frequency hysteresis current control for VSI inverters with simple feedforward bandwidth prediction", IEEE Trans. Industry Appl. vol 33, no. 5 pp. 1194-1202
- [10] C.T. Chen, Linear System Theory and Design, Oxford University Press, 3rd Edition, 1999
- [11] I. Cervantes, D. Garcia, D Noriega, (2003) "Linear control of quasi-resonant converters" IEEE Trans. Power Electronics, vol. 18, no. 5, pp.1194-1201.,
- [12] J. Alvarez-Ramirez and G. Espinosa-Perez, (2002) "Stability of current-mode control for DC-DC power converters", System & Control Lett. vol 45 pp. 113-119.

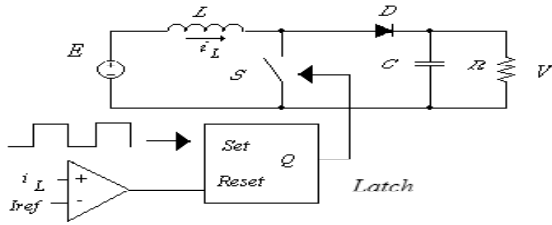


Figure 1. Boost converter

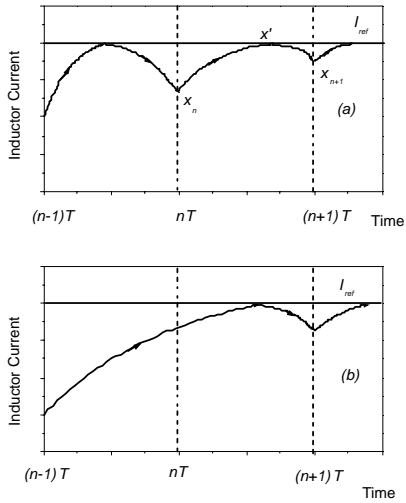


Figure 2. Typical current waveforms of the converter under CPC.

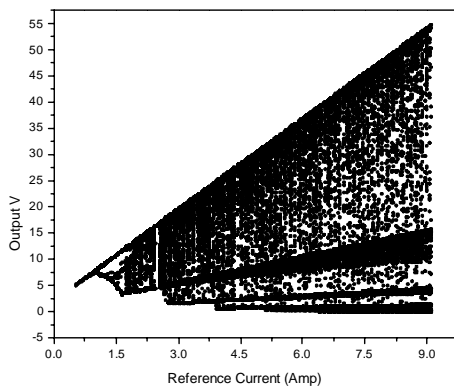


Figure 3. Bifurcation digram with reference current as parameter.

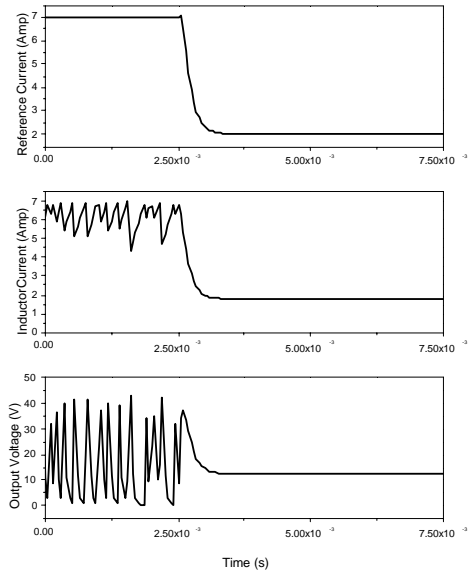


Figure 4. Time evolution of the system with the proposed controller.

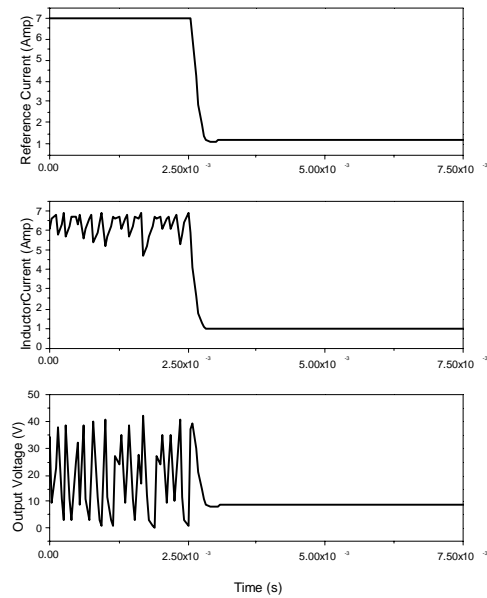


Figure 5. Time evolution of the system with the proposed controller in presence of parametric uncertainty.